Received: 12 December 2017
DOI: 10.1002/mop.31264

Controllable and wide spurious suppression power divider with a bandpass-filtering and high isolation

Phirun Kim | **Girdhari Chaudhary** | **Yongchae Jeong**

Division of Electronics and Information Engineering, IT Convergence Research Center, Chonbuk National University, Jeonju, Republic of Korea

Correspondence
Yongchae Jeong, Division of Electronics and Information Engineering, IT Convergence Research Center, Chonbuk National University, Jeonju, Republic of Korea.
Email: ycjeong@jbnu.ac.kr

Funding information
Ministry of Education, Science and Technology, Korea, Grant/Award Number: 2016R1D1A1B03931400; Korean Research Fellowship Program through the National Research Foundation (NRF) of Korea; Ministry of Science, ICT and Future Planning, Grant/Award Numbers: 2016H1D3A1938065

Abstract

This article presents a bandpass-filtering power divider with a controllable and wide spurious frequency. The proposed structure consists of four stepped-impedance resonators (SIR) that are directly coupled to the output ports of the power divider with an electrical length of θ. The spurious frequency can be controlled by changing the ratio of the SIR. Moreover, the isolation resistor provides an effective isolation between the output ports and an effective output return loss over wide stopbands. For the experiment validation, the power dividers with the stepped-impedance ratios of 0.83 and 1.43 were designed, fabricated, and measured at the center frequency of 2.6 GHz. The measured results are in good agreement with the simulated results.

KEYWORDS

bandpass filter, coupled lines, isolation, power divider, spurious frequency, stepped-impedance resonator

1 | INTRODUCTION

Bandpass filtering power divider are multifunctional radio frequency (RF) circuits that are widely used in antenna arrays, amplifiers, and mixers to divide/combine RF signals, reduce the junction loss of several path circuits, and enhance the stopband characteristics.

Figure 1A shows the conventional equal-split Wilkinson power divider.[1] The circuit is simple to design in terms of microstrip technology; however, the selectivity capabilities around the passband and stopband attenuations are poor. These issues can be solved by integrating the bandpass filters (BPFs) into the output ports of the divider,[2,3] as shown in Figure 1B; however, the overall circuit size was enlarged and caused additional losses. In recent years, filtering power dividers with various structures and techniques for which the multiresonator,[4-6] the multimode resonator,[7-12] and multistub transmission lines (TLs) are used[13-15] have been proposed. In Refs. [4] and [5], miniaturized multiresonator bandpass-filtering power dividers are proposed for which a net-type resonator with two open- and short-ended stubs is used. Similarly, a bandpass-filtering power divider was designed using four coupled quarter-wavelength (λ/4) resonators with four shunt open stubs provided wide-stopband characteristics.[6] In Ref. [7], a wide passband-filtering power divider was designed using a multi-mode resonator with limited out-of-band suppression characteristics. Alternatively, wide-stopband-filtering power dividers with multimode resonators and shunt-open/short-stub TLs were introduced in Refs. [8–12], while several transmission zeros were produced in the stopband by using the same TLs. In Ref. [13], a bandpass-filtering power divider was designed by cascading a π-type impedance-matching network with a large circuit size for which the third harmonic ($3f_0$) was retained. In Ref. [14], a shunt-configuration open-circuit-stub lowpass-filtering power divider was designed. The wide-stopband was suppressed by three transmission zeros; however, the selectivity near the passband is poor. A wideband-filtering power divider that is based on the coupled-line sections and open/short-circuit stubs is presented in Ref. [15]. Moreover, an unequal termination- impedance power divider was

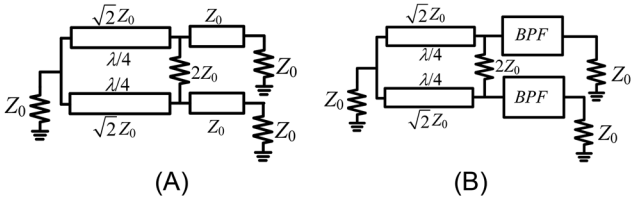

FIGURE 1 A, Conventional equal-split Wilkinson power divider[1] and B, Wilkinson power divider with a BPF at the output ports.[2,3]

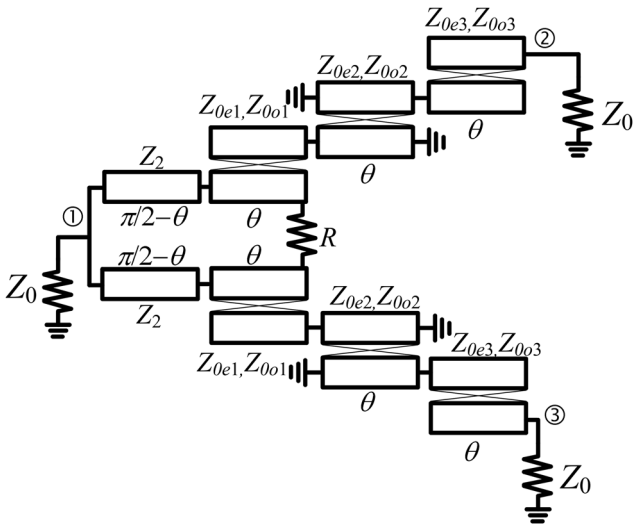

FIGURE 2 Configuration of the proposed bandpass filtering power divider

discussed in Ref. [16]. To improve the stopband characteristics, unequal termination-impedance power dividers with a bandpass-filtering response were designed by using a coupled-line section, open-stub TLs,[17] and two cascaded parallel coupled lines.[18] The filtering power dividers with the wide passband, wide-stopband, high isolation, and an unequal termination impedance have been presented using different structures; however, a filtering power divider with a controllable and wide spurious frequency has not been studied.

In this article, a microstrip-technology bandpass-filtering power divider with a high isolation is presented analytically with a controllable and wide spurious frequency. A low ratio of a stepped-impedance resonator (SIR) is given the broadest spurious-free bandwidth. To verify the design analysis, two prototypes of the bandpass-filtering power dividers were designed, fabricated, and measured with different-ratios SIRs.

2 | ANALYSIS

Figure 2 shows the structure of the proposed bandpass-filtering power divider. The circuit consists of a pair of two SIRs. A resistor (R) is connected at the open ends of the output dividing TLs. The SIRs are directly coupled to the output ports of the divider with an electrical length of θ. Thus, the circuit size and the insertion loss can be reduced compared with those of Refs. [2] and [3]. Since the proposed circuit is symmetrical, an even- and odd-mode analysis can be applied. The scattering parameters of the equal-split power dividers are expressed in terms of even- and odd-mode scattering parameters, as given by the following Equations of 1[19]:

$$S_{11}=S_{11e}=S_{22e}, \tag{1a}$$

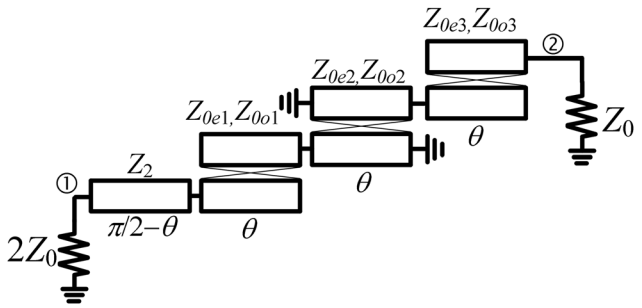

FIGURE 3 Schematic of an even-mode circuit

$$S_{12}=S_{21}=S_{31}=S_{13}=\frac{S_{21e}}{\sqrt{2}}, \tag{1b}$$

$$S_{22}=S_{33}=\frac{S_{22e}+S_{22o}}{2}, \tag{1c}$$

$$S_{23}=S_{32}=\frac{S_{22e}-S_{22o}}{2}, \tag{1d}$$

where the subscripts e and o denote the even and odd modes, respectively.

2.1 | Even-mode excitation and its equivalent circuits

From (1a) and (1b), the desired bandpass-filtering response with a matched terminated impedance should be obtained in the even mode. Thus, when the input signal is driven at the port 1 and terminated with the matched impedance, the power is not dissipated at the resistor. Figure 3 illustrates the even-mode equivalent circuits that consist of two-stage SIRs with the electrical parameters Z_2, Z_{0ei}, and Z_{0oi} (i = 1, 2, and 3) and an electrical length of θ. The design parameters were derived from the filter synthesis. At this mode, the source termination impedance becomes $2Z_0$, but R does not affect the connected circuit. The equivalent circuit of the even-mode circuit is depicted in Figure 4 with alternative J/K inverters. The Z_1 and Z_2 are the characteristic image impedances of the short- and open-end coupled lines, respectively. The impedance values of the termination impedances need to be the same at the input and output ports of the power divider, thereby setting $Z_2 = Z_0$. In Figure 4, the source-input admittance (Y_{S_e}) and the load-input admittance (Y_{L_e}) can be derived as (2a) and (2b), respectively, as follows:

$$Y_{S\_e}=2Y_0, \tag{2a}$$

$$Y_{L\_e}=Y_0. \tag{2b}$$

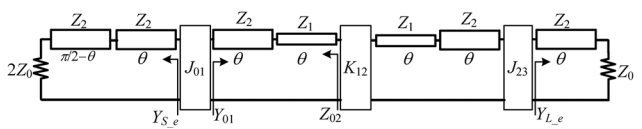

FIGURE 4 Equivalent circuit of an even-mode circuit

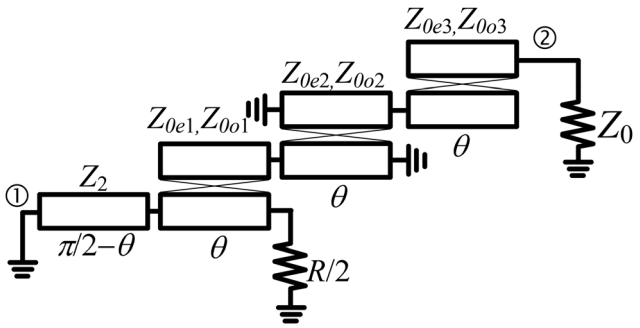

FIGURE 5 Schematic of an odd-mode circuit

From Figure 4, the resonator input admittance and impedance are defined as (3a) and (3b), respectively, as follows:

$$Y_{01} = jB = jY_2 \frac{\tan^2\theta - R_Z}{\tan\theta(1+R_Z)}, \tag{3a}$$

$$Z_{02} = jX = jZ_1 \frac{\tan^2\theta - R_Z}{\tan\theta(1+R_Z)}, \tag{3b}$$

where R_Z is the SIR of the resonator ($R_Z = Z_2/Z_1 = Y_1/Y_2$).

From (3), the resonator slope parameters are given as (4a) and (4b),[20] respectively, as follows:

$$b = \frac{\theta_0}{2}\frac{dB}{d\theta}\bigg|_{\theta=\theta_0} = \theta_0 Y_2, \tag{4a}$$

$$x = \frac{\theta_0}{2}\frac{dX}{d\theta}\bigg|_{\theta=\theta_0} = \theta_0 Z_1, \tag{4b}$$

where

$$\theta_0 = \tan^{-1}\sqrt{R_Z}. \tag{5}$$

The reactance (X) and the susceptance (B) are the imaginary parts of the Y_{01} and Z_{02}, respectively. And θ_0 is the electrical length at f_0. The resonator length and the spurious frequencies can be controlled by changing the R_Z. The relationship between the R_Z and the spurious resonance frequencies is presented in Refs. [20] and [21].

Using (4), the admittance and impedance inverter can be calculated using (6), as follows:

$$J_{01} = \sqrt{\frac{2Y_0 b_1 \mathrm{FBW}}{g_0 g_1}} = Y_0\sqrt{\frac{2\theta_0 \mathrm{FBW}}{g_0 g_1}}, \tag{6a}$$

$$K_{12} = \mathrm{FBW}\sqrt{\frac{x_1 x_2}{g_1 g_2}} = Z_1 \mathrm{FBW}\theta_0\sqrt{\frac{1}{g_1 g_2}}, \tag{6b}$$

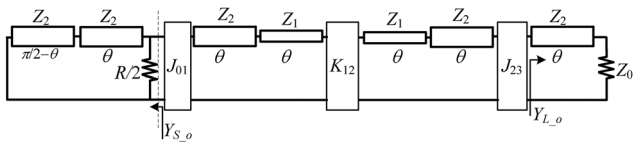

FIGURE 6 Equivalent circuit of an odd-mode circuit

$$J_{23} = \sqrt{\frac{Y_0 b_2 \mathrm{FBW}}{g_2 g_3}} = Y_0\sqrt{\frac{\theta_0 \mathrm{FBW}}{g_2 g_3}}, \tag{6c}$$

where FBW is a fractional bandwidth, and g_0, g_1, g_2, and g_3 are the lowpass-filter-prototype elements that can be defined as either equal-ripple or maximally flat characteristics. The conditions of $b_1 = b_2 = b$ and $x_1 = x_2 = x$ can be obtained from (4a) and (4b), respectively. The impedances and admittances of the even- and odd-mode characteristics of the coupled lines were calculated using (7) for the coupled line with the open-end stub, and (8) is used for the coupled line with the short-end stub,[21] as follows:

$$Z_{0e(1,3)} = Z_2 \frac{1 + J_{(01,23)}Z_2\csc\theta_0 + \left(J_{(01,23)}Z_2\right)^2}{1 - \left(J_{(01,23)}Z_2\right)^2\cot^2\theta_0}, \tag{7a}$$

$$Z_{0o(1,3)} = Z_2 \frac{1 - J_{(01,23)}Z_2\csc\theta_0 + \left(J_{(01,23)}Z_2\right)^2}{1 - \left(J_{(01,23)}Z_2\right)^2\cot^2\theta_0}, \tag{7b}$$

and

$$Y_{0e(2)} = \frac{1}{Z_{0e(2)}} = Y_1 \frac{1 - K_{12}Y_1\csc\theta_0 + (K_{12}Y_1)^2}{1 - (K_{12}Y_1)^2\cot^2\theta_0}, \tag{8a}$$

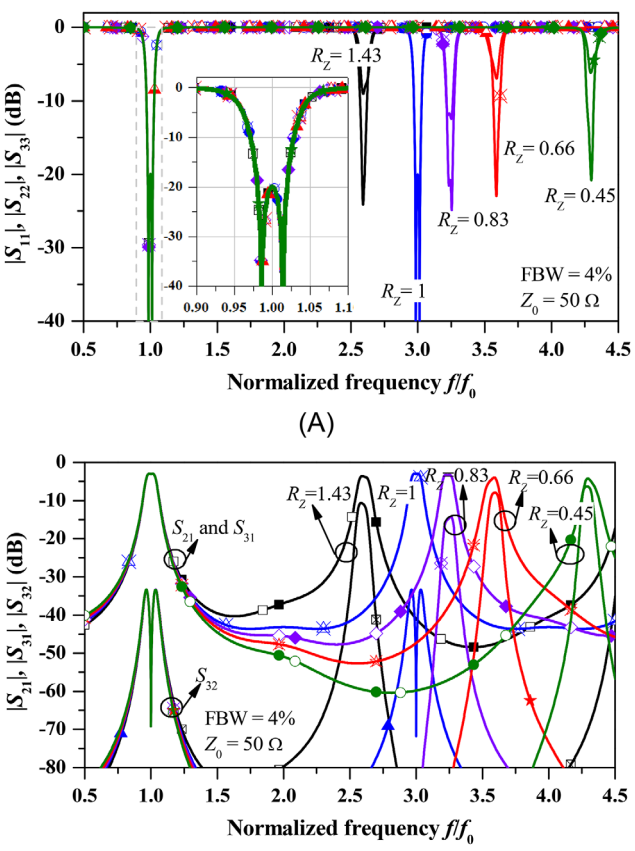

FIGURE 7 *S*-parameter characteristics with different R_Z values: (A) input/output return losses and (B) insertion loss and isolation [Color figure can be viewed at wileyonlinelibrary.com]

TABLE 1 Design parameters for the power divider with different R_Z values

f = f_0 = l, ripple = 0.043 dB, FBW = 4%, Z0 = 50 Ω						
J_{01}	K_{12}	J_{23}	θ(°)	R (Ω)	Z1 (Ω)	RZ
0.006477	2.029291	0.00458	50.082	50	35	1.43
0.006139	2.604811	0.004341	45	50	50	1
0.005959	2.94462	0.004214	42.392	50	60	0.83
0.005733	3.406356	0.004054	39.231	50	75	0.66
0.005336	4.328226	0.003773	33.988	50	110	0.45

$$Y_{0o(2)} = \frac{1}{Z_{0o(2)}} = Y_1 \frac{1 + K_{12}Y_1 \csc\theta_0 + (K_{12}Y_1)^2}{1 - (K_{12}Y_1)^2 \cot^2\theta_0}. \quad (8b)$$

2.2 | Odd-mode excitation and its equivalent circuits

Under the odd-mode excitation, the equivalent circuit of the proposed power divider is shown in Figure 5. In this mode, the source termination is short-circuited and R is divided in half; therefore, the equivalent circuit of Figure 5 is depicted in Figure 6. Consequently, the network section between J_{01} and the load is identical to that of the network in Figure 4, where the related variables are calculated using (6)–(8). At f_0, the λ/4 TL of the Z_2 with a short-circuit stub is transformed into that of an open circuit at the resistor junction. Then, Y_{S_o} is set to Y_{S_e} for the matching of the output ports. As a result, an effective output return loss and isolation characteristics were obtained simultaneously. When $Y_{S\_e} = Y_{S\_o}$, the isolation resistor was found as

$$R = Z_0. \quad (9)$$

2.3 | Controllable spurious power divider

Design examples were performed to verify the design formulas. From the even- and odd-mode analysis, the bandpass-filtering equal-split power divider with the controllable spurious frequency was designed with different R_Z values. The dividers are designed for FBW = 4% with an equal ripple of 0.043 dB ($S_{11} = -20$ dB @ f_0). In this case, the ideal elements are used to simulate the theoretical performance of the proposed power divider using the advance design system (ADS).

Figure 7 shows the *S*-parameter characteristics of the return/insertion losses and the isolations of the proposed power divider with different R_Z values. The spurious frequency was moved to a high frequency from 2.59 f_0 to 4.3 f_0 when the R_Z was decreased from 1.43 to 0.45, as shown in Figure 7A. Moreover, the passband return-loss characteristics are almost same for all of the R_Z values. The insertion-loss and isolation characteristics are depicted in Figure 7B. The stopband-attenuation characteristics are improved as the R_Z was decreased. A perfect isolation was obtained at f_0 for all of the R_Z values. All of the designed parameters in Figure 7 are listed in Table 1. The lengths of the resonators were also shortened as the R_Z was decreased. A low R_Z implies a small circuit size; however, the *J*/*K*-inverter values were decreased/increased, thereby causing a realization difficulty of the coupled lines.

3 | SIMULATION AND MEASUREMENT RESULTS

The design examples of the proposed power divider were implemented on a substrate of the RT/Duriod 5880 with $\varepsilon_r = 2.2$ and $h = 0.787$ mm. The power dividers were designed to operate at $f_0 = 2.6$ GHz with FBW = 4%, $R_Z = 0.83$ and 1.43, and ripple = 0.043 dB. The calculated *J*/*K* inverters are listed in Table 1. Using (7) and (8), the even- and odd-mode characteristic impedances of the coupled TLs were calculated and are listed in Table 2. The widths, spacings, and lengths of the resonators were

TABLE 2 Calculated even- and odd-mode impedance for the power divider with different R_Z values

*f*0 = 2.6 GHz, ripple = 0.043 dB, FBW = 4%, Z0 = R = 50 Ω								
Z0e1 (Ω)	Z0o1 (Ω)	Z0e2 (Ω)	Z0o2 (Ω)	Z0e3 (Ω)	Z0o3 (Ω)	θ (°)	Z1 (Ω)	Rz
88.26	36.28	38.29	31.71	73.33	38.34	42.39	60	0.83
85.66	36.19	64.35	55.64	71.66	38.65	50.082	35	1.43

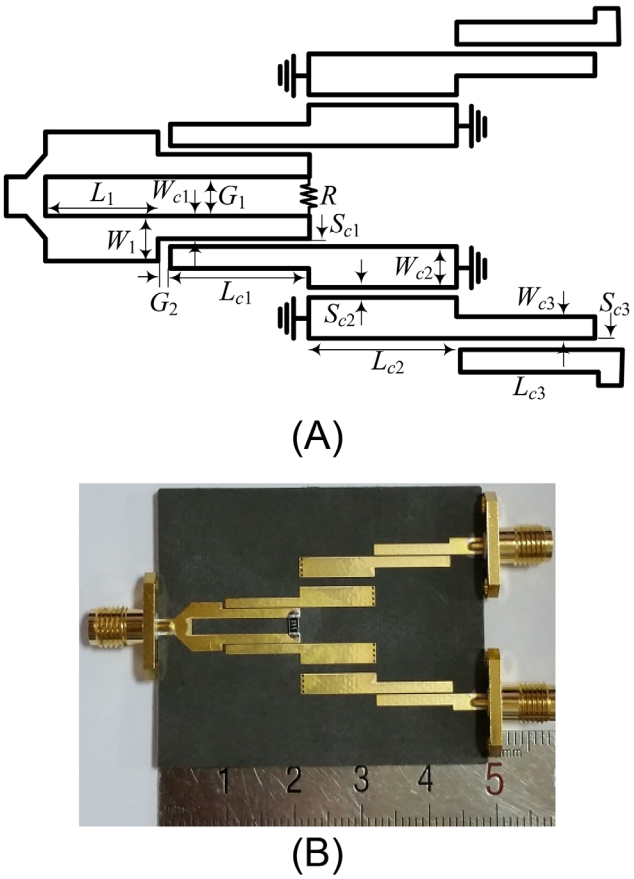

FIGURE 8 Proposed power divider I: (A) layout and (B) photograph of the fabricated circuit [Color figure can be viewed at wileyonlinelibrary.com]

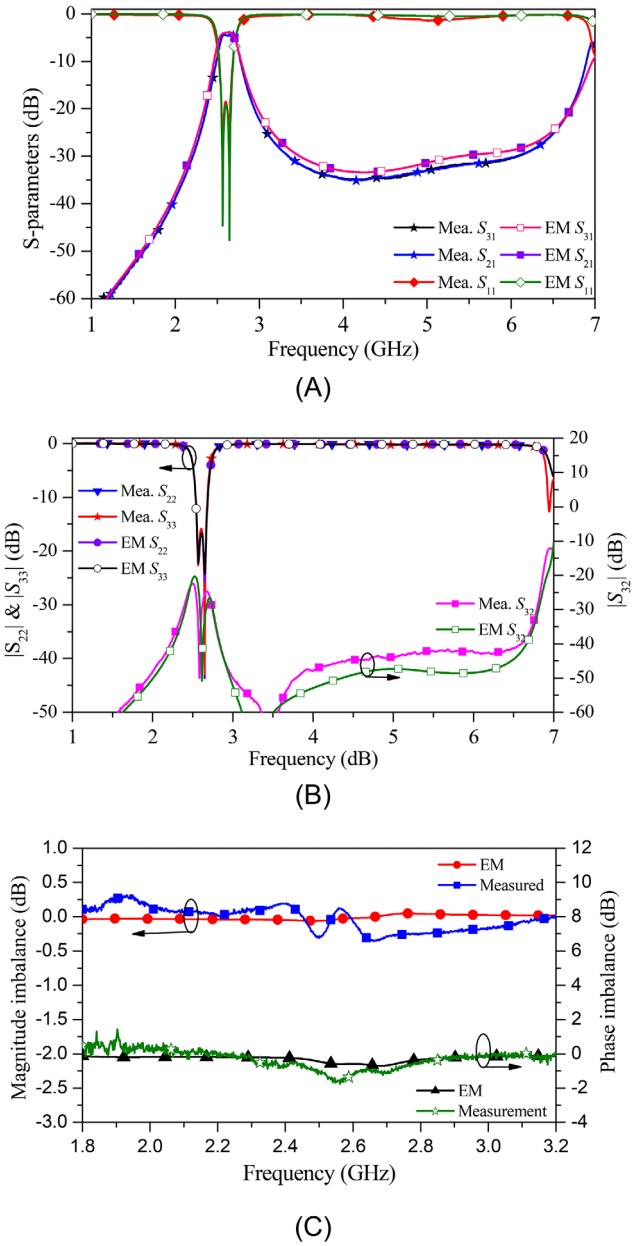

FIGURE 9 Simulated and measured results of the proposed power divider: (A) magnitudes of S_{11}, S_{21}, and S_{31}, (B) magnitudes of S_{22}, S_{33}, and S_{32}, and (C) phase and magnitude imbalances [Color figure can be viewed at wileyonlinelibrary.com]

calculated using LineCalc from the ADS tool. The electromagnetic simulation was performed using the ANSYS HFSS.

The photograph of the fabricated circuit and the layout of the power divider I are shown in Figure 8 with $R_Z = 1.43$. The fabricated layout data are listed in Table 3. The overall circuit size of the proposed power divider is 41.1 × 25.48 mm^2 (0.49λ_g × 0.3λ_g), where λ_g is a guided wavelength of 50 Ω microstrip lines at f_0. The simulated and measured *S*-parameter characteristics of the proposed power dividers are shown in Figure 9. The measured return and insertion losses ($|S_{21}|$ and $|S_{31}|$) were better than 18.5 dB and 0.95 dB at f_0, respectively, as shown in Figure 9A. Moreover, the input return loss was better than 18.5 dB from 2.54 to 2.65 GHz. The spurious frequency occurred at 7 GHz (2.69f_0) in the case of $R_Z = 1.43$. The stopband attenuations are better than 25 dB from dc to 2.29 GHz at the lower band and from 3.08 to 6.52 GHz at the higher band. Figure 9B shows the characteristics of the output return loss and the isolation. The measured output return loss is better than 16 dB within the passband; furthermore, the measured isolation is

TABLE 3 Physical dimensions of the fabricated power divider I

$W_1 = 2.4$	$Sc1 = 0.1$	$G_2 = 0.5$	$L_{c2} = 11.2$	$L_{c3} = 11.3$
$L1 = 4.5$	$L_{c1} = 11.6$	$Wc2 = 3$	$Wc3 = 1.6$	R = 56Ω
$Wc1 = 1.4$	$G1 = 2.4$	$S_{c2} = 1.4$	$Sc3 = 0.24$	

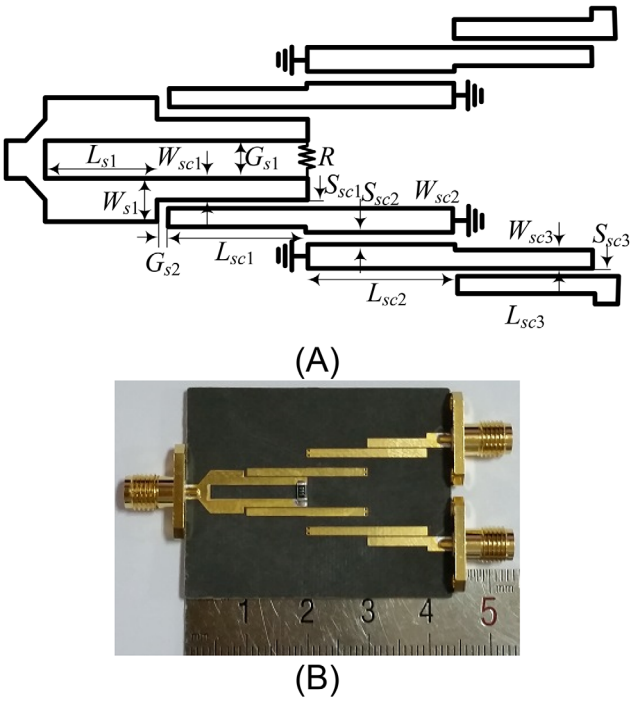

FIGURE 10 Proposed power divider II: (A) layout and (B) photograph of the fabricated circuit [Color figure can be viewed at wileyonlinelibrary.com]

better than 22 dB from dc to 6.85 GHz. Figure 9C shows the simulated and measured magnitude and phase imbalance characteristics. The measured magnitude and phase imbalances are <0.4 dB and 1.4° within a wide band, respectively.

The fabricated circuit and the layout of the power divider II are shown in Figure 10 with $R_Z = 0.83$. The fabricated-layout data are listed in Table 4. The overall circuit size of the proposed power divider is 37.65 × 19.82 mm^2 ($0.45\lambda_g \times 0.23\lambda_g$). The simulated and measured *S*-parameter characteristics of the proposed power dividers are shown in Figure 11. The measured return and insertion losses are better than 24 and 0.97 dB at f_0, respectively, as shown in Figure 11A. The measured bandwidth of the input return loss is better than 22 dB from 2.54 to 2.64 GHz. The spurious frequency occurred at 8.6 GHz ($3.3f_0$), which is much higher location than of the power divider I. The stopband attenuations are better than 25 dB from dc to 2.19 GHz at the lower band and from 3.15 to 8.16 GHz at the higher band. Figure 11B shows the characteristic of the output return loss and the isolation. The measured output return loss was better than 16.5 dB within the passband. The measured isolation is better than 20 dB from dc to 9 GHz. Figure 11C shows the simulated and

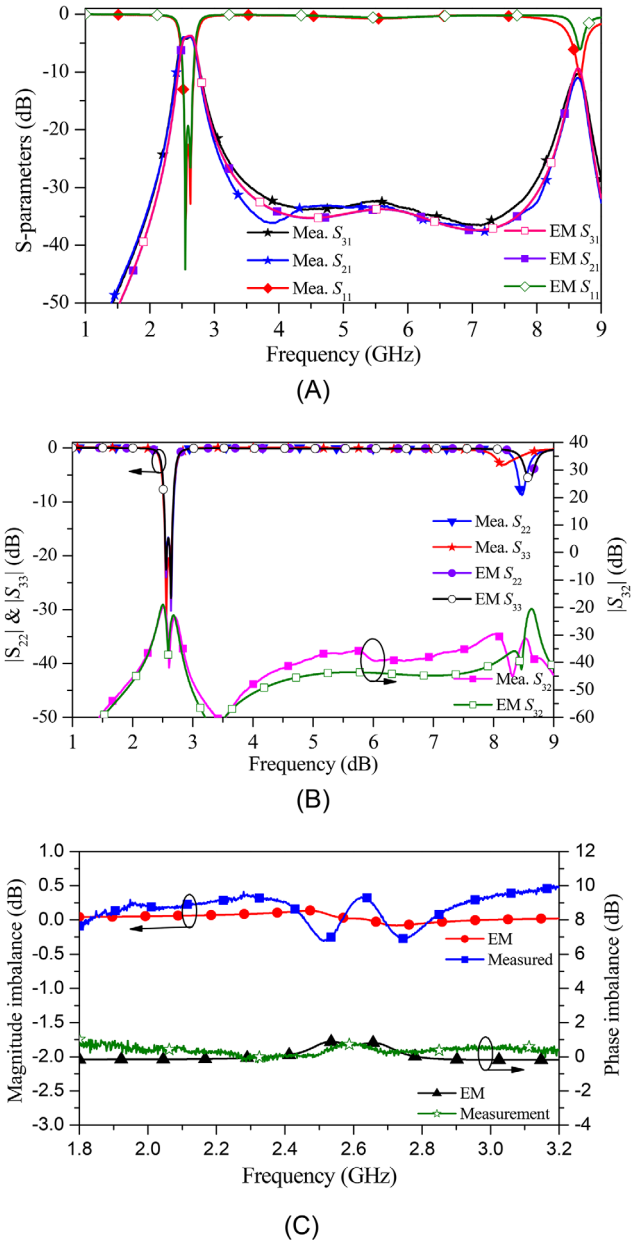

FIGURE 11 Simulated and measured results of the proposed power divider: (A) magnitudes of S_{11}, S_{21}, and S_{31}, (B) magnitudes of S_{22}, S_{33}, and S_{32}, and (C) phase and magnitude imbalances [Color figure can be viewed at wileyonlinelibrary.com]

measured magnitude and phase imbalances between the two output ports. The measured magnitude and phase imbalances are <0.43 dB and 1.1° within a wide band, respectively.

Table 5 shows the performance comparison regarding the proposed power divider and the previous work. The proposed

TABLE 4 Physical dimensions of the fabricated power divider II

Ws1 = 2.4	*S*sc1 = 0.1	*G*s2 = 0.5	L_{sc2} = 10	L_{sc3} = 9.8
Ls1 = 5.5	L_{sc1} = 10.35	*W*sc2 = 1.4	*W*sc3 = 1.5	R = 56 Ω
*W*sc1 = 1.33	*G*s1 = 2.4	S_{sc2} = 1.8	Ssc2 = 0.18	

TABLE 5 Performance comparison of the proposed filtering power divider and the other work

	*f*0 (GHz)	ILmax (dB)	$S_{11}/S_{22}/S_{33}$ (dB)	S_{32} (dB)	Spurious
[3]	1.5	1.5	N.A	22.4 (DC to 2.9 GHz)	UC
[5]	1.2	1.4	16/≅14/≅15	>30 (0.9 to 1.5 GHz)	UC
[6]	1.4	1.3	15/25/25	>16 (DC to 5 GHz)	UC
[7]	2.24	0.45	15.7/≅14/≅14	>22.5 (1 to 3.5 GHz)	UC
[8]	2.42	1.6	18/15/N.A	>20 (at 2.42 GHz)	UC
[9]	3.7	0.85	20/20/20	>17 (at 3.7 GHz)	UC
[10]	2.4	0.97	21.6/N.A/N.A	>22 (DC to 7.5 GHz)	UC
[11]	1.568	1.6	15/15/N.A	>10 (≅1.5 to 1.63 GHz)	UC
[12]	1	1.2	15/24/N.A	>17 (≅0.95 to 1.05 GHz)	UC
This work I	2.6	0.95	18.5/16/16	>22 (DC to 6.85 GHz)	C
This work II	2.6	0.97	24/16.5/16.5	>20 (DC to 9 GHz)	C

Abbreviations: UC, uncontrollable; C, controllable; ILmax, maximum insertion loss.

work is advantageous due to its controllable spurious frequency, high isolation, and wide-stopband characteristics.

4 | CONCLUSION

In this paper, a bandpass-filtering power divider with a controllable spurious frequency, good isolation, and wide spurious suppression characteristics is presented using SIRs. The resonators are directly coupled to λ/4 TLs with an electrical length of θ. For the experiment validation, equal-split power dividers with Chebyshev bandpass responses were designed and fabricated in a microstrip line. The measured results are good agreement with the simulated and analytical results. The design equations were derived based on a coupled-line bandpass-filter theory. The proposed network is simple to design in terms of microstrip technology, and its applicability for wireless communication systems is expected.

ACKNOWLEDGMENT

This research was supported by the Basic Science Research Program through the NRF of Korea, funded by Ministry of Education, Science and Technology (2016R1D1A1B03931400) and partially supported by the Korean Research Fellowship Program through the National Research Foundation (NRF) of Korea, funded by the Ministry of Science, ICT and Future Planning (2016H1D3A1938065).

ORCID

Phirun Kim http://orcid.org/0000-0002-3889-8253

REFERENCES

[1] Pozar D. *Microwave Engineering*. 4th ed. New York, NY: Wiley; 2012.

[2] Deng PH, Dai LC. Unequal Wilkinson power dividers with favorable selectivity and high-isolation using coupled-line filter transformers. *IEEE Trans Microw Theory Tech.* 2012;60(6):1520–1529.

[3] Deng PH, Chen Y. New Wilkinson power dividers and their integration applications to four-way and filtering dividers. *IEEE Trans Compon Packag Manuf Technol.* 2014;4(11):1828–1837.

[4] Chen Huang C, Shen TT, Wu R. Design of miniaturized filtering power dividers for system-in-a-package. *IEEE Trans Compon Packag Manuf Technol.* 2013;3(10):1663–1672.

[5] Chen C, Lin C. Compact microstrip filtering power dividers with good in-band isolation performance. *IEEE Microw Wireless Compon Lett.* 2014;24(1):17–19.

[6] Zhao X, Gao L, Zhang X, Xu J. Novel filtering power divider with wide stopband using discriminating coupling. *IEEE Microw Wireless Compon Lett.* 2016;26(8):580–582.

[7] Wang X, Wang J, Zhang G. Design of wideband filtering power divider with high selectivity and good isolation. *Electron Lett.* 2016;52(16):1389–1391.

[8] Song K, Hu S, Mo Y, Fan Y, Zhong C. Novel bandpass-response power divider with high frequency selectivity using centrally stub-loaded resonators. *Microwave Opt Technol Lett.* 2013;55(7):1560–1562.

[9] Ren X, Song K, Hu B, Chen Q. Compact filtering power divider with good frequency selectivity and wide stopband based on composite right-/left-handed transmission lines. *Microwave Opt Technol Lett.* 2014;56(9):2122–2125.

[10] Zhang G, Wang J, Zhu L, Wu W. Dual-mode filtering power divider with high passband selectivity and wide upper stopband. *IEEE Microw Wireless Compon Lett.* 2017;27(7):642–644.

[11] Wei F, Ding C, Li J, Wang X, Shi X. Compact filtering power divider with improved out-of-band performance. *Microwave Opt Technol Lett.* 2015;57(10):2274–2277.

[12] Chen C, Ho Z. Design equations for a coupled-line type filtering power divider. *IEEE Microw Wireless Compon Lett.* 2017;27(3):257–259.

[13] Chao S, Lin W. Filtering power divider with good isolation performance. *Electron Lett.* 2014;50(11):815–817.

[14] Cheng KM, Ip W. A novel power divider design with enhanced spurious suppression and simple structure spurious suppression and simple structure. *IEEE Trans Microw Theory Tech.* 2010;58(12):3903–3908.

[15] Wu Y, Zhuang Z, Liu Y, Deng L, Ghassemlooy Z. Wideband filtering power divider with ultra-wideband harmonic suppression and isolation. *IEEE Access.* 2016;4:6876–6882.

[16] Ahn H, Wolff I. Three-port 3-dB power divider terminated by different impedances and its application to MMIC's. *IEEE Trans Microw Theory Tech.* 1999;47(6):786–794.

[17] Kim P, Jeong J, Chaudhary G, Jeong Y. A design of unequal termination impedance power divider with filtering and out-of-band suppression characteristic. In: Proceeding of 45th European Microwave Conference. Paris; 2015:123–126.

[18] Kim P, Chaudhary G, Jeong Y. Analysis and design of an unequal termination impedance power divider with bandpass filtering response. *Electron Lett.* 2017;53(18):1260–1262.

[19] Ahn H. *Asymmetric Passive Components in Microwave Integrated Circuit*. Wiley, Hoboken, NJ; 2006:155–167.

[20] Makimoto M, Yamashita S. *Microwave Resonators and Filters for Wireless Communication: Theory, Design, and Application*. New York: Springer-Verlag Berlin Heidelberg; 2001:65–106.

[21] Makimoto M, Yamashita S. Bandpass filters using parallel coupled stripline stepped impedance resonators. *IEEE Trans Microw Theory Tech.* 1980;28(12):1413–1417.

How to cite this article: Kim P, Chaudhary G, Jeong Y. Controllable and wide spurious suppression power divider with a bandpass-filtering and high isolation. *Microw Opt Technol Lett*. 2018;60:1862–1869. https://doi.org/10.1002/mop.31264

Received: 14 December 2017

DOI: 10.1002/mop.31256

A filtering impedance transformer with high transforming ratio

Shiyong Chen | **Meng Li** | **Yantao Yu** | **Mingchun Tang**

College of Communication Engineering, Chongqing University, Chongqing, China

Correspondence
Chen Shi-Yong, College of Communication Engineering, Chongqing University, Chongqing 400044, China.
Email: chensy@cqu.edu.cn

Funding information
National Natural Science Foundation of China, Grant/Award Numbers: 61571069 and 61471072; the Fundamental Research Funds for the Central Universities, Grant/Award Number: 106112017CDJQJ168817

Abstract

A filtering impedance transformer with high transforming ratio and good suppression out of band is presented in this article. Design parameters of the proposed configuration are analyzed. For verification, a 50 to 500 Ω transformer operating at 3 GHz has been designed, fabricated, and measured. The measured maximum insertion is about 0.87 dB and the measured return loss is better than 18 dB from 2.71 to 3.29 GHz, which are in good agreements with the simulated ones.

KEYWORDS

coupled line, impedance transformer, transmission zeros

1 | INTRODUCTION

The impedance transformer is one of the fundamental circuits used in wireless communication systems and can be applied in design of power dividers, filters, and amplifiers. A traditional impedance transformer with quarter wavelength can provide a narrow bandwidth as it is only matched at the center frequency. In order to broaden the operating bandwidth, coupled transmission line and coupled three-line are utilized to design impedance transformers.[1–5] But the rejection at stopband is poor. To enhance the selectivity, a parallel coupled line with an open shunt stub is introduced.[6] The wider return loss bandwidth is achieved by keeping the parallel coupled line in over-matched condition. Moreover, two transmission zeros (Tzs) around the passband is generated to improve suppression characteristics. However, impedance transforming ratio is <3. To solve this problem, two cascaded coupled lines are used to obtain ultra-high impedance transforming ratio and filtering response simultaneously.[7,8] However, there is no transmission zeros around the passband, which leads to poor selectivity.

In this article, a filtering impedance transformer with ultra-high transforming ratio based on coupled lines with short circuited ends is presented. The proposed impedance transformer exhibit a wide operating bandwidth and good selectivity as two transmission zeros out of band is generated. A prototype is designed, fabricated, and measured. The